This article was downloaded by: [University of Colorado at Boulder Libraries]
On: 15 August 2012, At: 14:01
Publisher: Taylor & Francis
Informa Ltd Registered in England and Wales Registered Number: 1072954 Registered office: Mortimer House, 37-41 Mortimer Street, London W1T 3JH, UK

HVAC&R Research
Publication details, including instructions for authors and subscription information:
http://www.tandfonline.com/loi/uhvc20

Spatial distribution of fluence rate from upper-room ultraviolet germicidal irradiation: Experimental validation of a computer-aided design tool

Stephen N. Rudnick [a] , Melvin W. First [a] , Tim Sears [b] , Richard L. Vincent [c] , Philip W. Brickner [c] , Peter Y. Ngai [d] , John Zhang [e] , Robert E. Levin [f] , Kenneth Chin [g] , Ronald O. Rahn [h] , Shelly L. Miller [i] & Edward A. Nardell [j]

[a] Department of Environmental Health, Harvard School of Public Health, 665 Huntington Ave., Boston, MA, 02115-6021, USA

[b] Acuity Brands Lighting, One Lithonia Way, Bldg. 3, Conyers, GA, 30012, USA

[c] Department of Medicine, Mount Sinai School of Medicine, General Internal Medicine, Section of Community Medicine, One Gustav L. Levy Place, Box 1087, New York, NY, 10029, USA

[d] Acuity Brands Lighting, 2246 5th Street, Berkeley, CA, 94710, USA

[e] Lunera, 3696 Haven Avenue, Suite A, Redwood City, CA, 94063, USA

[f] Retired from OSRAM SYLVANIA, 42 Lions Lane, Salem, MA, 01970, USA

[g] Tufts University, Boston, MA, 02115, USA

[h] School of Public Health, University of Alabama Birmingham, 1665 University Blvd South, Birmingham, AL, 35294, USA

[i] Department of Mechanical Engineering, Environmental Engineering Program, 427 UCB, University of Colorado, Boulder, CO, 80309-0427, USA

[j] Harvard Medical School (Medicine; Global Health and Social Medicine), Harvard School of Public Health (Environmental Health; Immunology and Infectious Diseases), Brigham and Women's Hospital, Division of Global Health Equity, FXB Building, 709c, 651 Huntington Ave., Boston, MA, 02115, USA

Accepted author version posted online: 02 May 2012. Version of record first published: 10 Aug 2012

To cite this article: Stephen N. Rudnick, Melvin W. First, Tim Sears, Richard L. Vincent, Philip W. Brickner, Peter Y. Ngai, John Zhang, Robert E. Levin, Kenneth Chin, Ronald O. Rahn, Shelly L. Miller &

Edward A. Nardell (2012): Spatial distribution of fluence rate from upper-room ultraviolet germicidal irradiation: Experimental validation of a computer-aided design tool, HVAC&R Research, 18:4, 774-794

To link to this article: http://dx.doi.org/10.1080/10789669.2012.667863

PLEASE SCROLL DOWN FOR ARTICLE

Full terms and conditions of use: http://www.tandfonline.com/page/terms-and-conditions

This article may be used for research, teaching, and private study purposes. Any substantial or systematic reproduction, redistribution, reselling, loan, sub-licensing, systematic supply, or distribution in any form to anyone is expressly forbidden.

The publisher does not give any warranty express or implied or make any representation that the contents will be complete or accurate or up to date. The accuracy of any instructions, formulae, and drug doses should be independently verified with primary sources. The publisher shall not be liable for any loss, actions, claims, proceedings, demand, or costs or damages whatsoever or howsoever caused arising directly or indirectly in connection with or arising out of the use of this material.

Downloaded by [University of Colorado at Boulder Libraries] at 14:01 15 August 2012

Taylor & Francis
Taylor & Francis Group

Spatial distribution of fluence rate from upper-room ultraviolet germicidal irradiation: Experimental validation of a computer-aided design tool

Stephen N. Rudnick,[1] Melvin W. First,[1] Tim Sears,[2] Richard L. Vincent,[3,*] Philip W. Brickner,[3] Peter Y. Ngai,[4] John Zhang,[5] Robert E. Levin,[6] Kenneth Chin,[7] Ronald O. Rahn,[8] Shelly L. Miller,[9] and Edward A. Nardell[10]

[1]*Department of Environmental Health, Harvard School of Public Health, 665 Huntington Ave., Boston, MA 02115-6021, USA*
[2]*Acuity Brands Lighting, One Lithonia Way, Bldg. 3, Conyers, GA 30012, USA*
[3]*Department of Medicine, Mount Sinai School of Medicine, General Internal Medicine, Section of Community Medicine, One Gustav L. Levy Place, Box 1087, New York, NY 10029, USA*
[4]*Acuity Brands Lighting, 2246 5th Street, Berkeley, CA 94710, USA*
[5]*Lunera, 3696 Haven Avenue, Suite A, Redwood City, CA 94063, USA*
[6]*Retired from OSRAM SYLVANIA, 42 Lions Lane, Salem, MA 01970, USA*
[7]*Tufts University, Boston, MA 02115, USA*
[8]*School of Public Health, University of Alabama Birmingham, 1665 University Blvd South, Birmingham, AL 35294, USA*
[9]*Department of Mechanical Engineering, Environmental Engineering Program, 427 UCB, University of Colorado, Boulder, CO 80309-0427, USA*
[10]*Harvard Medical School (Medicine; Global Health and Social Medicine), Harvard School of Public Health (Environmental Health; Immunology and Infectious Diseases), Brigham and Women's Hospital, Division of Global Health Equity, FXB Building, 709c, 651 Huntington Ave., Boston, MA 02115, USA*
[*]*Corresponding author e-mail: richard.vincent@mountsinai.org*

Downloaded by [University of Colorado at Boulder Libraries] at 14:01 15 August 2012

A commercial computer-aided design tool used by the lighting industry was modified to predict fluence rates for upper-room ultraviolet germicidal irradiation. Experimental validation based on more than 1600 measurements and 3 types of commercial ultraviolet fixtures, which was done in an experimental chamber and in a homeless shelter having fixtures in continuous use for over 7 years, showed differences in measured and predicted average upper-room fluence rates of less than 10%. The computer-aided design tool, however,

Received June 2, 2011; accepted February 2, 2012

Stephen N. Rudnick, DSc, CIH, is Lecturer on Industrial Hygiene Engineering. **Melvin W. First, DSc, PE, CIH**, is Professor of Environmental Health Engineering, Emeritus. **Tim Sears, MIES**, is Senior Illuminating Engineer. **Richard L. Vincent, FIES, LEED-AP**, ASHRAE Member, is Administrative Manager. **Philip W. Brickner, MD**, is Director of Tuberculosis Studies. **Peter Y. Ngai, PE, FIES, LC**, is Vice President of Research and Development. **John Zhang, MIES, LC**. **Robert E. Levin, PhD**, is Corporate Scientist (Retired). **Kenneth Chin** is Medical Student. **Ronald O. Rahn, PhD**, is Adjunct Professor of Environmental Health Science. **Shelly L. Miller, PhD**, is Associate Professor. **Edward A. Nardell, MD**, is Associate Professor.

HVAC&R Research, 18(4):774–794, 2012. Copyright © 2012 ASHRAE.
ISSN: 1078-9669 print / 1938-5587 online
DOI: 10.1080/10789669.2012.667863

was not very successful at predicting fluence rates at specific room locations, a capability that is needed for mating computational fluid dynamics with ultraviolet germicidal irradiation. Although not an objective of this study, it was also found that the three types of fixtures used in this study have surprisingly significant differences in efficiency based on fixture ultraviolet power output and electrical input. One fixture type had an efficiency that was more than five times that of another. For comparison purposes, a standard method for measuring and reporting fixture efficiency is needed.

Downloaded by [University of Colorado at Boulder Libraries] at 14:01 15 August 2012

Introduction

Background

Airborne transmission of infectious agents is a significant threat to global health because of the efficiency with which infectious particles can spread within crowded congregate settings, such as hospitals, clinics, homeless shelters, jails, prisons, and refugee camps. Pulmonary tuberculosis (TB), a disease contracted exclusively by airborne transmission, is one of today's top two fatal infections of adults worldwide—the other being HIV/AIDS (Dye and Floyd 2006). The emergence of multidrug-resistant TB and extensively drug-resistant strains not only imperils global TB control, but also may reverse the health gains achieved by the worldwide expansion of antiretroviral therapy for HIV/AIDS (Gandhi et al. 2006). Other infectious agents with substantial potential for airborne transmission include influenza, SARS, measles, and potential bioterrorism agents, such as smallpox and anthrax (Roy and Milton 2004; Rudnick and First 2007; Brickner et al. 2003).

Engineering control of airborne infectious agents is an important strategy for reducing airborne transmission of disease vectors. Various methods are available, including general dilution ventilation, personalized ventilation that protects an individual's microenvironment (Pantelic et al. 2009), in-duct air cleaners, in-room air cleaners, and upper-room ultraviolet germicidal irradiation (UVGI). Of these, upper-room UVGI has some unique advantages; it has the potential to process large quantities of room air relatively inexpensively, rapidly, and without noise. General dilution ventilation, except under ideal conditions, is expensive, because large quantities of conditioned air must be exhausted outdoors. In-duct air cleaners provide clean air for general dilution ventilation and have the same disadvantages. To be effective, in-room air cleaners must process large quantities of air, resulting in noise generation, utilization of valuable space, and considerable electrical energy consumption, in order to move large quantities of air through an air-cleaning device.

UVGI utilizes 254-nm ultraviolet (UV) radiation from low-pressure mercury discharge lamps to reduce the indoor concentration of infectious agents. UVGI damages the genetic material of microorganisms so that they are unable to replicate. Beginning in the 1930s (Wells 1955; Riley and O'Grady 1961) and continuing to the present day (Xu et al. 2003, 2005; First et al. 2007; NIOSH 2009), numerous experimental studies have demonstrated the effectiveness of upper-room UVGI for reducing the airborne concentration of culturable microorganisms. Recently, Escombe et al. (2009) demonstrated the effectiveness of upper-room UVGI by exposing guinea pigs to air extracted from TB patient rooms with UV fixtures that were either turned on or off.

The primary objective of upper-room UVGI is to indirectly disinfect the air in the lower, occupied portion of a room so that airborne transmission of pathogens from infected to exposed occupants is reduced. When applying upper-room UVGI, the air in the upper room is irradiated while UV radiation in the lower portion of the room is kept below levels that may be harmful to occupants. Because of these competing goals, it is generally necessary to have the UV radiation pass through deep, closely spaced horizontal louvers before entering the room. Unfortunately, these louvers significantly reduce the effectiveness of upper-room UVGI. A secondary objective of upper-room UVGI is to disinfect return air so that pathogen transmission in other rooms ventilated by the same air handing unit will also be reduced. This latter objective can be more fully realized when the return air grill is in the upper room; if it is in the lower room, disinfection of return air will be very dependent on vertical air mixing.

Because both infected and exposed occupants reside in the lower room, sufficient vertical air circulation is essential for upper-room UVGI to be effective. Thus, both air circulation between the upper and lower room and the amount of UV radiation

Downloaded by [University of Colorado at Boulder Libraries] at 14:01 15 August 2012

supplied to the upper room have a profound influence on the effectiveness of UVGI. Depending on environmental conditions, either of these parameters can be the controlling factor (Rudnick and First 2007). Because vertical air circulation in most rooms tends to be unreliable, the use of a ceiling fan, either blowing upward or downward depending on outdoor conditions, is highly recommended (NIOSH 2009).

The present article addresses the determination of the amount of UV radiation in the upper room provided by multiple UV fixtures and its spatial distribution. Three approaches were taken: (1) measurements in an experimental chamber with various types of instrumentation and methodologies, (2) measurements using a cylindrical sensor in a homeless shelter where UVGI had been in continuous operation for many years, and (3) predictions using a computer-aided design (CAD) tool. CAD tools for the interior lighting industry are widely available, but without modification, none can be used to predict the UV radiation field produced by louvered UV fixtures designed for upper-room UVGI. Therefore, one of the available CAD tools used by the lighting industry was modified for this purpose. As this study was originally conceived, measurements in an experimental chamber would be used to validate predictions by the CAD tool, and measurements in a homeless shelter would serve to confirm this validation under real-world conditions. In order to prevent bias, measurements and predictions, which were done independently by research groups at different locations, were submitted to a third party at a third location, after which comparisons were made.

Measurement of UV irradiance and fluence rate

In general, irradiance is defined as the UV power received on a surface divided by the area of that surface. Three different measures of irradiance, all having the same unit (e.g., $\mu W/cm^2$), are relevant to the present work: (1) planar irradiance, (2) cylindrical irradiance, and (3) spherical irradiance. Planar irradiance is generally referred to simply as irradiance, and spherical irradiance is usually called fluence rate, and this practice will be followed hereafter in this article.

Irradiance (planar) at a specific point is defined as the UV power per unit area received on one side of an infinitesimally small flat surface on which the specified point resides. Irradiance is directional; it includes UV radiation received over 2π steradians; that is, half of the possible directions from which UV rays might originate is included. Flat sensors, which are used for measurement of UV irradiance, are commercially available. The surface of the sensor is cosine corrected, so that the sensor will detect the UV power of radiation multiplied by the cosine of the angle that the ray makes with the surface of the sensor. Uncorrected sensors do not give a true measure of irradiance. These flat UV sensors are appropriate for measuring UV radiation in the lower room where the major concern is the amount of UV radiation that potentially could reach the eyes of occupants.

Cylindrical irradiance at a specific point is defined as the UV power per unit area received on the outer curved surface of an infinitesimally small cylinder centered at the specified point divided by the cylinder's cross-sectional area along its length, which is rectangular. Cylindrical irradiance is less directional than irradiance; it includes UV radiation over essentially 4π steradians; that is, all of the possible directions from which UV rays might originate are included. The influence of UV rays within a single plane that is perpendicular to the axis of the cylinder does not depend on direction. The influence of UV rays within different planes perpendicular to the axis of the cylinder, however, does depend on direction. UV sensors with a cylindrical shape are commercially available for measurement of cylindrical irradiance.

Fluence rate at a specific point is defined as the UV power per unit area received on the outer surface of an infinitesimally small sphere centered at the specified point divided by the sphere's cross-sectional area. Fluence rate is wholly non-directional and includes UV radiation over 4π steradians; that is, all of the possible directions from which UV rays might originate are included, and the influence of UV radiation received by the specified point is independent of direction. Fluence rate is considered to be the best measure of the UV radiation reaching an aerosol particle containing an infectious agent. Unfortunately, spherical UV sensors are not commercially available. A device based on chemical actinometry, however, can be used to measure fluence rate. Rahn (1997) and Rahn et al. (1999) exposed small-diameter hollow quartz spheres filled with a solution of KI and KIO_3 to UV radiation for a predetermined exposure time. Based on the change in absorbance of the solution after UVGI exposure, which can be measured with a

Downloaded by [University of Colorado at Boulder Libraries] at 14:01 15 August 2012

spectrophotometer, and on the exposure time, a true measure of fluence rate can be determined. This method for measuring fluence rate can be somewhat time consuming, particularly when fluence rate is low, because the lower the fluence rate, the longer the exposure times must be to provide sufficient sensitivity. In addition, if the solution is overexposed, a valid measurement will not be obtained. Until recently, this method was most useful as a research tool. Minor modifications in the methodology, however, can make it a relatively convenient technique for use in the field (Rahn and Echols 2010).

Provided that the surface of the flat sensor is held perpendicular to a line from the source to the sensor, measurements with a flat sensor can also be used to estimate fluence rate provided three conditions are met: (1) there is a single UV source; (2) reflections from room surfaces, particularly those that are not within the 2π steradian viewing angle of the flat sensor, are not significant; and (3) the sensor is not too close to the source. When the sensor is too close to the UV source—which, for practical purposes, is when the distance from the sensor to the source is on the order of the size of the largest linear dimension of the source—the fluence rate will be underestimated by a flat sensor. For multiple UV fixtures in a room, measurements for each fixture can be taken with a flat sensor while the other fixtures are turned off. The sum of these measurements can then be used as an estimate of fluence rate.

If the axis of a cylindrical sensor is held perpendicular to a line from the source to the sensor, measurements with a cylindrical sensor can also be used to estimate fluence rate. For a cylindrical sensor, however, the conditions that need to be met will be less stringent than for a flat sensor: (1) measurement of fluence rate for multiple sources may be feasible; (2) reflections from room surfaces will be received over a 4π steradian viewing angle; and (3) when the UV source is a linear lamp, a cylindrical sensor allows measurements to be made significantly closer to the source than a flat sensor provided the sensor is properly oriented. For example, if the axis of the linear source is horizontal, which is generally the case, and the axis of the cylindrical sensor is vertical, then the length of the linear lamp will not influence how close to the source measurements can be taken; instead, the diameter of the lamp will be the controlling distance.

Fluence rate can also be determined by measuring and summing the planar irradiances on four faces of a tetrahedron (Björn 1995). Similarly, fluence rate has been determined by measuring and summing the irradiances on the faces of a cube (Schafer et al. 2008), but according to Björn (1995), this latter method is incorrect. Nonetheless, the measurements of Schafer et al. (2008) agreed reasonably well with actinometrical measurements.

Materials and methods: Experimental chamber

Description

The experimental chamber, which is located on the roof of a five-story building, has a 10 ft by 15 ft (3.05 m by 4.57 m) floor and a 10-ft-high (3.05-m) ceiling. The floor is covered with vinyl tiles, and the walls and ceiling are covered with a pebbled, hard-finish, white plastic wallboard. The reflectivity of this wallboard was measured to be 10% at 254 nm. When viewed in a dark room under UV light, however, the fluorescence of the plastic wallboard was obvious. Because the reflectivity was measured with a Lambda 900 spectrophotometer (Perkin Elmer, Waltham, MA), an instrument with a single monochromator located before the sample, any radiation due to fluorescence would have been included as reflectivity at the excitation wavelength; thus, the true reflectivity is less than 10%.

UV fixtures

Measurements were made in the experimental chamber with three different UV fixture configurations:

1. Two Hygeaire model LIND 24-EVO wall fixtures (Atlantic Ultraviolet Corp., Hauppauge, NY), each containing one 25-W linear lamp, sat on a shelf with its bottom surface at a height of 89 in. (2.26 m) above the floor and the back of the fixture 0.6 in. (15.2 mm) from the wall. One wall fixture was located on one short wall, and the other wall fixture on the other short wall. One side of each fixture was 2 ft (0.610 m) away from a long wall, but the fixtures were not facing each other (see Figure 1). Hygeaire fixtures have an electronically variable ballast that allows the UV output to be adjusted. During all tests, the UV output was set to its maximum value.
2. One Lumalier model CM-218 corner fixture (Commercial Lighting Design, Inc., Memphis, TN) containing two 18-W folded compact lamps

Downloaded by [University of Colorado at Boulder Libraries] at 14:01 15 August 2012

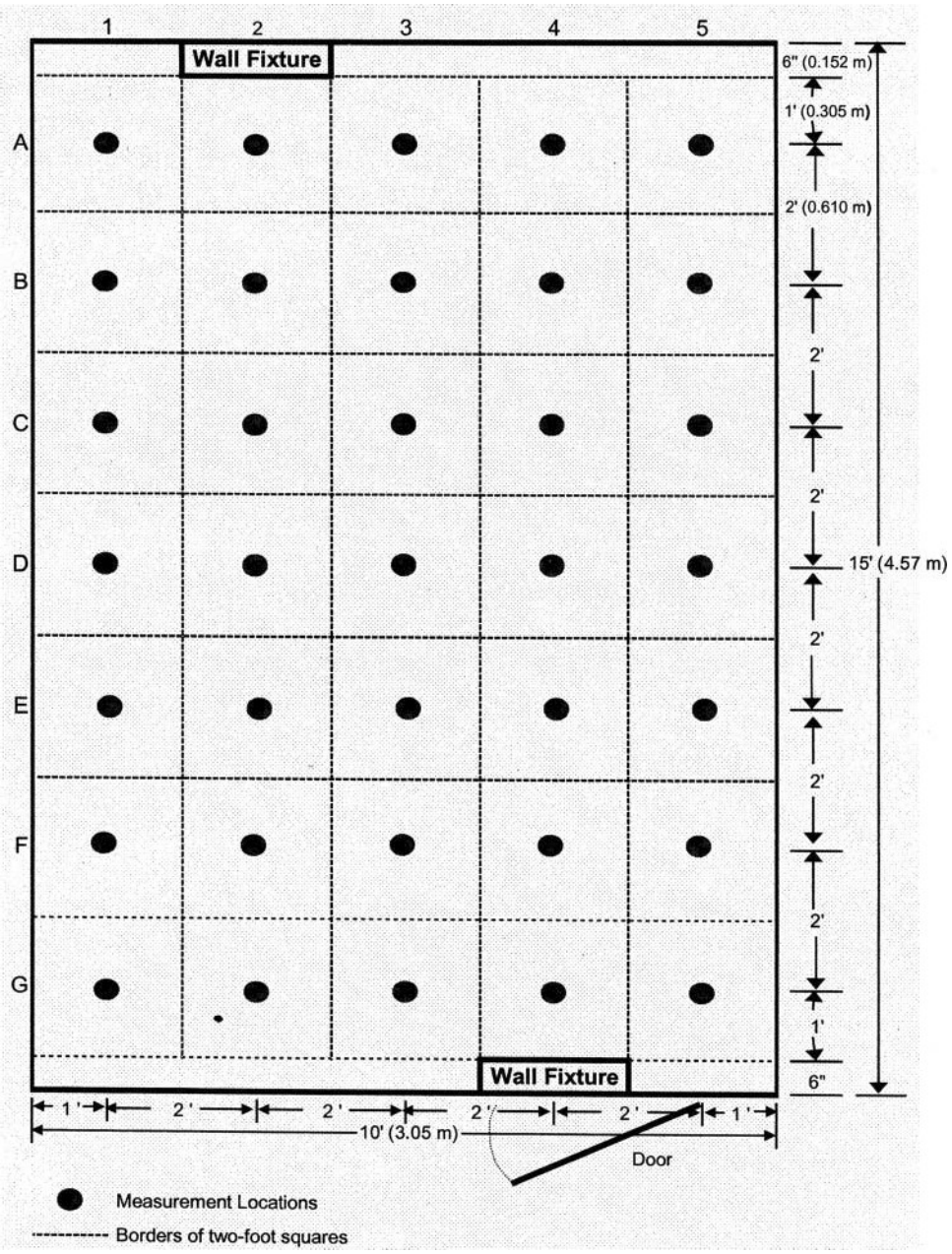

Figure 1. Horizontal measurement grid.

was mounted with its bottom surface at a height of 83.5 in. (2.12 m) above the floor in each of the four corners of the chamber.

3. The same four Lumalier model CM-218 corner fixtures plus one Lumalier model PM-418 pendant fixture (Commercial Lighting Design, Memphis, TN), a horizontally omni-directional fixture containing four 18-W folded compact lamps, hung from the geometric center of the ceiling with its bottom surface at a height of 82.5 in. (2.10 m) from the floor.

All of the Lumalier fixtures had ballasts that cannot be adjusted to vary UV output. The tops of all fixtures were leveled so that the angle that the louvers make with the top of the fixture, which is set

Downloaded by [University of Colorado at Boulder Libraries] at 14:01 15 August 2012

by the manufacturer, and the angle at which the UV beam rises relative to the horizontal plane would be the same. New lamps were installed in all fixtures; the fixtures were then turned on and allowed to operate continuously for about 2 weeks prior to taking any measurements.

Measurement methods

A horizontal measurement grid, which is shown in Figure 1, was defined for the purpose of horizontally positioning the UV sensors and the hollow quartz spheres used for chemical actinometry in the space containing the direct UV rays emitted by the fixtures. The experimental chamber's floor, not including the space within 6 in. (0.152 m) of both short walls, which for simplicity was ignored, was subdivided into 35 2-ft (0.610 m) squares, each containing 4 1-ft (3.05 m) square vinyl tiles. The centers of these 35 2-ft (0.610 m) squares, which correspond to the intersection of the 4 vinyl floor tiles, was used as the horizontal measurement grid. Measurement points are designated in Figure 1 by row, which are labeled A, B, C, D, E, F, and G, and by column, which are labeled 1, 2, 3, 4, and 5.

A plum bob attached to the center of the bottom of a tripod and nearly touching the floor was used to horizontally position the flat or cylindrical sensors, which were mounted at the center of the top of the tripod. For the hollow quartz spheres, the string from which they were suspended was carefully aligned with the horizontal center of the tripod. In order to position the sensors vertically, the tripod was marked so that the sensors could be positioned at predetermined heights above the floor. These heights were chosen so as to essentially straddle the UV beam. Similarly, the hollow quartz spheres were suspended from the ceiling of the experimental chamber by a string such that their centers were located at the desired heights.

Measurements using flat sensor

Measurements of irradiance were made using a GigaHertz-Optik model P9710 optometer and a model UV-3718–2 flat UV sensor (Puchheim, Germany). According to the manufacturer, the optometer has an accuracy of $\pm 0.2\%$; the flat UV sensor has a relative calibration uncertainty of $\pm 6.5\%$ and low-end resolution of 6 nW/cm^2 (60 μW/m^2). A small laser pointer was mounted onto the side of the flat sensor, such that the laser beam would be perpendicular to the face of the sensor. When irradiance measurements were being made, the laser beam was directed at the geometric center of the fixture's louvers to ensure that the sensor was properly positioned. Measurements were made only while a single UV fixture was turned on—either the wall fixture closest to the door (see Figure 1), the corner fixture located in the back right corner of the chamber (top right corner in Figure 1), or the pendant fixture. At heights of 7, 7.5, 8, 8.5, 9, and 9.5 ft (2.13, 2.29, 2.44, 2.59, 2.74, and 2.90 m) for the wall fixture and 6, 6.5, 7, 7.5, 8, and 8.5 ft (1.83, 1.98, 2.13, 2.29, 2.44, and 2.59 m) for the corner fixture, irradiance measurements were made at all 35 test sites, which are indicated by solid circles in the horizontal measurement grid shown in Figure 1. At heights of 6, 6.5, 7, 7.5, 8, and 8.5 ft (1.83, 1.98, 2.13, 2.29, 2.44, and 2.59 m) for the pendant fixture, only test sites in the upper left-hand quadrant of the chamber as shown in Figure 1 were measured; that is, measurements were made at 11 test sites located in both rows 3 through 5 and columns A through D with the exception of test sites located at 3D, which were occupied by the pendant fixture. Because of symmetry, the irradiance at locations in the other three quadrants was assumed to be identical to the upper left-hand quadrant.

In order to estimate the fluence rate for the simultaneous operation of the two wall fixtures mounted on opposite walls, as shown in Figure 1, two assumptions were required.

1. The irradiance field due to the wall fixture farthest from the door, which was not measured, was assumed to be identical to that due to the wall fixture closest to the door, which was measured. Although it would have been preferable to have measured the irradiance field for each fixture, all of the fixtures used in the chamber are well-made, look exactly the same, have the same model number, were purchased together, and had operated for essentially the same length of time.
2. Reflections from chamber surfaces were not significant and thus could be ignored. Because reflections, which are less than 10%, would be expected to be diffuse, much of the reflected UV radiation would likely not return to the irradiated zone and would not influence the measurements; thus, this latter assumption appears to be reasonable.

If both wall fixtures were operating, the fluence rate at a particular location was determined based on the principle of superposition; that is, the UV fields

Downloaded by [University of Colorado at Boulder Libraries] at 14:01 15 August 2012

from each fixture are superposed so that the irradiance at any location is the sum of the irradiances from each of the wall fixtures operating separately. In order to sum the two UV fields mathematically, the irradiance field was imagined to have been rotated 180° and then placed on top of the original irradiance field. The two irradiances at each of the test sites were then summed. The resultant values were used as estimates of the fluence rates at the test sites when two wall fixtures were operating simultaneously.

Estimating fluence rate for the simultaneous operation of four corner fixtures—one in each of the chamber's corner—based on measurement of the irradiance field from a single corner fixture, was done in an exactly analogous fashion. The irradiance field from a single corner fixture was imagined to have been rotated initially by 90°, then by 180°, and finally by 270°. These three rotated irradiance fields were placed on top of the original irradiance field. The four irradiances at each of the test sites were then summed. The resultant values were then used as estimates of the fluence rates at the test sites when four corner fixtures were operating simultaneously. Estimating fluence rate for the third fixture configuration—four corner fixtures and a pendant fixture—was done by summing the fluence field for the four corner fixtures and the irradiance field generated by the pendant fixture.

Measurements using cylindrical sensor

Measurements of cylindrical irradiance were made using a GigaHertz-Optik model P9710 optometer and a model ROD-360-UV18–2 cylindrical UV sensor (Puchheim, Germany). According to the manufacturer, the cylindrical UV sensor has a relative calibration uncertainty of ±6.5% and low-end resolution of 15 nW/cm^2 (150 μW/m^2). The cylindrical sensor was oriented such that its axis was always vertical; it would have been preferable to keep the axis of the cylindrical sensor always perpendicular to a line from the sensor to the center of the fixture's louvers, but this is not possible when multiple fixtures are operating.

Although the cylindrical sensor comes closest to measuring cylindrical irradiance, the measured value was used as an estimate of fluence rate. Louvered UV fixtures emit a vertically narrow, nearly horizontal beam. With the axis of the cylindrical sensor vertical, its response due to UV rays that are perpendicular to its axis are the same as for a spherical sensor. The farther the UV rays are from being perpendicular to the sensor's axis, however, the poorer this estimate becomes. Nevertheless, if the sensor is a sufficiently far enough distance from the fixture, a cylindrical sensor would be expected to yield a reasonable estimate of fluence rate.

All of the UV fixtures used for a specific fixture configuration were turned on when measurements were made with the cylindrical sensor. The measurement test sites, which are shown in Figure 1, depended on the fixture configuration being used.

1. When two wall fixtures were turned on, measurements were made at the 20 test sites located in both rows 1 through 5 and columns A through D for each of the six horizontal planes having heights of 7, 7.5, 8, 8.5, 9, and 9.5 ft (2.13, 2.29, 2.44, 2.59, 2.74, and 2.90 m) above the floor.
2. When four corner fixtures were turned on, measurements were made at the 12 test sites located in both rows 3 through 5 and columns A through D for each of 6 horizontal planes having heights of 6, 6.5, 7, 7.5, 8, and 8.5 ft (1.83, 1.98, 2.13, 2.29, 2.44, and 2.59 m) ft above the floor.
3. When four corner fixtures and one pendant fixture were turned on, measurements were made at 11 test sites located in both rows 3 through 5 and columns A through D, but not test site 3D, for each of six horizontal planes having heights of 6, 6.5, 7, 7.5, 8, and 8.5 ft (1.83, 1.98, 2.13, 2.29, 2.44, and 2.59 m) above the floor. No measurements were made at 3D because the pendant fixture occupied those test sites.

Cylindrical irradiances were not measured at the remainder of test sites shown in fixture #1, but they could be estimated based on symmetry.

Measurements using chemical actinometry

Iodide/iodate chemical actinometry was used to measure fluence while all of the UV fixtures used for a specific fixture configuration were turned on. The procedure was based on a methodology designed for use in the field (Rahn and Echols 2010). Hollow quartz spheres (10 mm [2.54 in.]) fully filled with a solution of KI and KIO_3 were used as a UV sensor. The absorbance of the resulting triiodide endpoint was measured with a handheld Hach #5870042 Pocket Colorimeter II Filter Photometer (Loveland, CO) having a 420-nm LED light source. This device was adapted to hold the spheres in the optical light path. This method had three advantages over the method used previously by Rahn

Downloaded by [University of Colorado at Boulder Libraries] at 14:01 15 August 2012

et al. (1999): (1) all measurements could be completed without bringing solutions back to the laboratory for analysis, (2) contents of the spheres did not need to be transferred to a cuvette for measurement of absorbance as is required for a conventional spectrophotometer, and (3) sphere volumes did not need to be measured.

Because chemical actinometry takes considerably more time than measurements using a flat or cylindrical sensor, particularly for low fluence rates, fewer than six horizontal planes were evaluated for each fixture configuration. The test sites, which are shown in Figure 1, depended on the fixture configuration being used.

1. When two wall fixtures were turned on, measurements were made at the 20 test sites located in both rows 1 through 5 and columns A through D for each of the horizontal planes having heights of 7 and 8 ft (2.13 and 2.44 m) above the floor. Due to a mistake, however, the measurement for 2A for a height of 7 ft was lost.
2. When 4 corner fixtures were turned on, measurements were made at the 12 test sites located in both rows 3 through 5 and columns A through D for each of the horizontal planes having heights of 7, 7.5, and 8 ft (2.13, 2.29, and 2.44 m) above the floor:
3. When 4 corner fixtures and 1 pendant fixture were turned on, measurements were made at 11 test sites located in both rows 3 through 5 and columns A through D, but not test site 3D, for each of the horizontal planes having heights of 7 and 7.5 ft (2.13 and 2.29 m) above the floor. No measurements were made at test site 3D because the pendant fixture occupied those locations.

Materials and methods: Sitting room of a homeless shelter

Room description

The sitting room of a homeless shelter in New York City, which is shown in a schematic diagram in Figure 2, has a 260 in. by 758 in. (6.60 m by 19.3 m) floor and a 132-in.-high (3.35-m) ceiling. The walls are composed of either painted concrete blocks or painted sheetrock, although lockers cover the lower sections of the two shorter walls. The room has a painted concrete ceiling and a terrazzo floor, which is divided into 225 equal-area rectangular subdivisions that have a length of 30.3 in. (0.770 m)

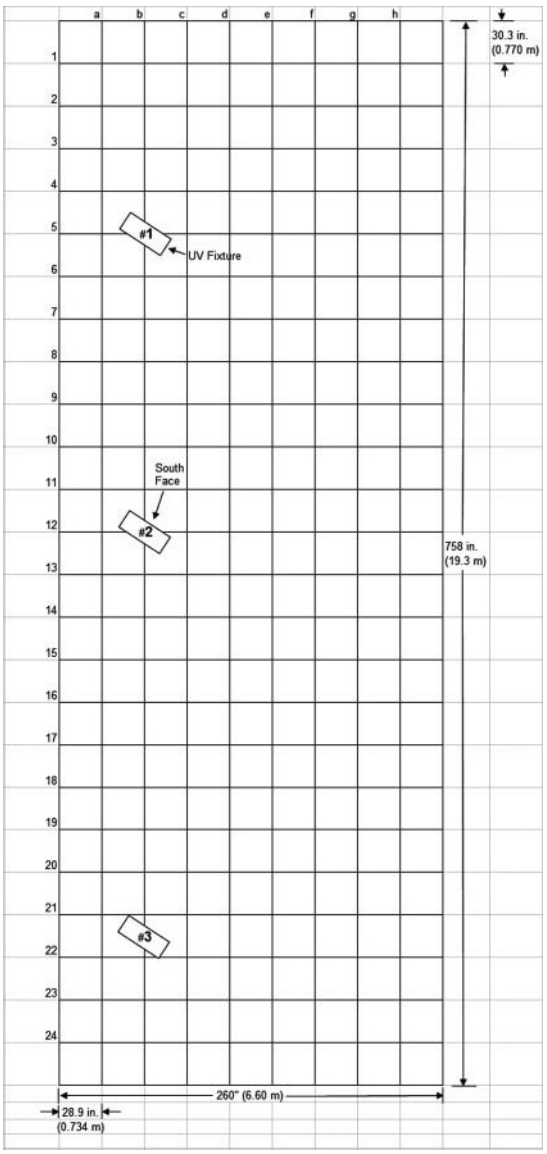

Figure 2. Top view of sitting room of New York City homeless shelter.

for the side parallel to the two longer walls and 28.9 in. (0.734 m) for the side parallel to the two shorter walls.

Fixture description

The sitting room contains three Hygeaire model LIND 24-EVO-2PM two-way pendant fixtures (Atlantic Ultraviolet Corp., Hauppauge, NY), each containing two 25-W UV linear lamps. These fixtures, which are hung from the ceiling, have been used continuously for over 7 years, although prior to

Downloaded by [University of Colorado at Boulder Libraries] at 14:01 15 August 2012

making measurements, new lamps were installed and allowed to operate continuously for about 2 weeks. These fixtures, labeled #1, #2, and #3 in Figure 2, have electronically variable ballasts that were adjusted to provide the maximum possible UV output during the tests. The fixtures are hung from the ceiling such that the bottom of fixtures #1, #2, and #3 are at a height above the floor equal to 103, 103.5, and 100 in. (2.62, 2.63, and 2.54 m), respectively. Their top surfaces were determined to be approximately horizontal. The faces of fixtures #1, #2, and #3 form angles of 42°, 38°, and 36°, respectively, with the long walls of the sitting room. These fixtures have two faces from which UV radiation is emitted horizontally in opposite directions. According to the manufacturer, each LIND 24-EVO-2PM two-way pendant fixture is exactly equivalent to back-to-back Hygeaire model LIND 24-EVO wall fixtures, the wall fixtures tested in this study's experimental chamber. Thus, for the purpose of predicting fluence rates, these fixtures were treated as back-to-back Hygeaire model LIND 24-EVO wall fixtures.

Methodology

Measurements

For the field study at the homeless shelter, the cylindrical sensor was chosen because it is much simpler and faster to use than either the flat sensor or chemical actinometry. Thus, all measurements were taken using the GigaHertz-Optik model P9710 optometer and model ROD-360-UV18–2 cylindrical UV sensor (Puchheim, Germany). The cylindrical sensor was positioned using the same procedures as in the experimental chamber. It was mounted on a tripod that had been marked to allow the sensor to be placed at a specified height with its axis always vertical. A plumb bob attached to the center of the bottom of the tripod and nearly touching the floor was used to position the sensor in the horizontal plane using a floor grid.

The horizontal measurement grid coincided exactly with the rectangular subdivisions of the terrazzo floor. Upper-room measurements were taken directly above the intersections of four rectangular subdivisions at heights of 96, 102, 108, 114, 120, and 126 in. (2.44, 2.59, 2.74, 2.90 3.05, and 3.20 m), above the floor. In Figure 2, the measurement sites in the horizontal plane are labeled by row ("1" through "24") and by column ("a" through "h"). This grid would be expected to result in a total of 1152 measurements for the 6 horizontal planes. However, due to the fixtures themselves and 2 ceiling beams, measurements could not be made at 2 points in each of the 3 lowest horizontal planes, 18 points in each of the 2 highest horizontal planes, and 10 points in the remaining plane, resulting in a total of 1100 measurements.

Benchmarking fixture output

Although new UV lamps had been installed in all fixtures prior to taking measurements, the fixtures themselves had been used continuously for more than 7 years. In order to benchmark these fixtures, the maximum irradiance on each side of the Hygeaire two-way pendant fixtures was measured at a distance of 3 ft (0.914 m) from the fixture's louvers. Specifically, for each face of the fixture, the horizontal and vertical planes that bisected the front of the fixture's louvers were found first. Their intersection 3 ft (0.914 m) away from the front edges of the louvers was the starting point where the center of the GigaHertz-Optik model UV-3718–2 flat UV sensor was placed. Keeping the sensor at a horizontal distance of 3 ft (0.914 m) from the front of the louvers and holding it parallel to the face of the fixture, the sensor was moved in all directions until the point of maximum irradiance was found, which was fairly close to the starting point.

Prediction of fluence rate using a CAD tool

By modifying Visual^{TM}(Acuity Brands Lighting, Conyers, GA), a commercially available CAD tool that is widely used by the lighting industry for analysis of architectural lighting layouts, its application was extended to the prediction of UV fluence rate where one or more highly collimated UV fixtures are used for upper-room UVGI. The CAD predictions for UVGI are based on the same algorithms used by Visual to perform calculations in the visible range of the spectrum. A description of Visual and the modifications that were necessary for use with fixtures designed for upper-room UVGI are given in the Appendix. Details regarding the fundamental equations upon which the CAD tool are based are given elsewhere (DiLaura 1982, 1996; DiLaura and Quinlan 1995). An updated version of the software, including modifications allowing it to be applied to upper-room UVGI, is available online at http://www.visual-3d.com/Downloads/Software/Setup/2010/Software.aspx. Instructional videos on the use of Visual can

Downloaded by [University of Colorado at Boulder Libraries] at 14:01 15 August 2012

be found at http://www.3d-visual.com/Training/Video/InstructionalVideos.asp.

In order to apply Visual, sources of UV radiation—specifically, highly collimated, upper-room fixtures for UVGI—must first be characterized in the laboratory by gonioradiometry, which is standard practice for lighting fixtures. A brief description of how gonioradiometry is done in the lighting industry and modifications that were necessary for gonioradiometry on fixtures designed for upper-room UVGI are in the Appendix. A more detailed description is given elsewhere (Zhang et al. 2012). Most laboratories that have the capability to do gonioradiometry on visible lighting fixtures are not presently set up to conduct gonioradiometry on fixtures used for upper-room UVGI.

Gonioradiometry was not done on all of the UV fixtures used in the experimental chamber and homeless shelter; only representative fixtures of the three model types that were used in this project were evaluated. The wall fixture used in the experimental chamber that was closest to the door, as shown in Figure 1, was assumed to be representative of both the Hygeaire model LIND 24-EVO wall fixtures used in the experimental chamber and the model LIND 24-EVO-2PM pendant fixtures used in the homeless shelter; thus, the pendant fixture was assumed to be equivalent to two back-to-back wall fixtures. The corner fixture located in the back right corner of the experimental chamber (top right corner in Figure 1) was assumed to be representative of the other three Lumalier model CM-218 corner fixtures used in the experimental chamber. Gonioradiometry was also done on the Lumalier model PM-418 pendant fixture used in the experimental chamber. Gonioradiometry is also an accurate way to characterize the UV power output of a fixture. If the electrical power input to the fixture is also measured, the overall efficiency of the fixture can be calculated.

When CAD predictions were compared with measurements taken with the flat UV sensor, the reflectivity of room surfaces was assumed to be 0%, because with only a single UV fixture turned on, the flat sensor would not be expected to detect much of the reflections from room surfaces. When CAD predictions were compared with measurements made with the cylindrical UV sensor and by chemical actinometry, the reflectivity of room surfaces was assumed to be 10%, because the cylindrical sensor and the quartz spheres used for chemical actinometry are able to detect all of the reflections from surfaces in the room. In that 10% reflectivity is not very significant relative to the direct UV radiation, lower values of reflectivity will not alter the CAD predictions much. For CAD predictions for the homeless shelter, 10% reflectivity is also a reasonable value because the walls and ceiling were painted. Although the reflectivity of the paint was not measured, most paints have a reflectivity at 254 nm of less than 10% (Ulrich and Evans 1976).

Statistical methods for validation of CAD tool

Comparison of measured and predicted average fluence rates

The choice of methodology for making a statistical comparison between the experimental measurements and predictions from the CAD tool depends on the objective. For design of an upper-room UVGI installation, NIOSH (2009) recommended that the average fluence rate in the upper room should be in the range of 30–50 μW/cm^2 (300–500 mW/m^2) based on research they sponsored at the University of Colorado (Miller et al. 2002). Because of this, the primary objective here was to compare measurement and prediction of average fluence rates in the upper room. Two related methods were used to make this comparison: (1) a paired *t*-test was used to determine whether the null hypothesis that the average difference between the measured and predicted fluence rates for each test site was equal to zero could be rejected (that is, was the average difference between a measurement and CAD prediction statistically significant at 95% confidence?) and 2) the average of the difference of the measured and predicted fluence rates and 95% confidence limits were determined; an overlap of these confidence limits is equivalent to a rejection of the null hypothesis.

Comparison of measured and predicted fluence rates at specific locations

Although the average fluence rate in the upper room is an important parameter for upper-room UVGI, prediction of fluence rate at a specific location in the upper room is also of considerable interest. Thus, experimental measurements and predictions from the CAD tool at specific locations in the upper room were also compared. A common procedure for evaluating agreement between a pair of numbers obtained by two different instruments or

Downloaded by [University of Colorado at Boulder Libraries] at 14:01 15 August 2012

methods is to make a scatter plot of one of the pairs versus the other and calculate a correlation coefficient. As pointed out by Altman and Bland (1983), this approach is misleading because it analyzes the strength of the relationship between the pair, not agreement. They instead proposed a graphical approach, which has been adapted for comparison of two fluence rates, one measured and the other obtained from a predictive model.

In the simplest form of this approach, the fluence rate, which is estimated as the average of a measured and predicted fluence rate, is plotted on the horizontal x-axis versus their difference on the vertical y-axis. The horizontal line, $y =$ mean difference, represents what is called the *bias line*. Perfect agreement between the two methods would correspond to a horizontal line coincident with the x-axis. Two other horizontal lines corresponding to the mean difference between the pairs ± 1.96 standard deviations of the differences are also plotted. These lines, which are called the *95% limits of agreement* (LOA), provide an interval within which 95% of the differences would be expected to lie. This type of plot, which has been widely used in the medical literature to compare two instruments or methods used for clinical measurements, is usually referred to as a Bland–Altman plot. How closely two methods must agree with each other to be acceptable requires judgment as to how close the agreement needs to be for a particular application.

One difficulty when determining fluence rate in the upper room using two different methods is that the values for fluence rate cover a large range. In general, the magnitudes of the difference increase as the fluence rate increases. Thus, rather than expecting a constant difference, the difference would be expected to be closer to directly proportional to the magnitude of the fluence rate. This suggests that the values should be log-transformed; that is, the Bland–Altman plot should be a plot of the difference between the logs of the values versus the average of the logs (Bland and Altman 1986). This turns out to be exactly equivalent to plotting the ratio of the two values on the vertical axis against their geometric mean on the horizontal axis, with logarithmic scales for both axes. When making this modified Bland–Altman plot, the 95% LOA cannot be specified in terms of the arithmetic mean ± 1.96 standard deviations. Rather, the 95% LOA will be given as the geometric mean multiplied or divided by a dimensionless factor equal to the geometric standard deviation raised to the 1.96 power.

Despite the use of the log-transformed values rather than the actual measured and predicted values, the magnitude of the differences between the log-transformed values may not be independent of the fluence rate. Thus, instead of using the arithmetic average value of the difference in the logs to define a horizontal bias line, the bias line can be obtained from a linear regression of the difference between the log of the values versus the arithmetic average of the log of the values (Bland and Altman 1999) or, equivalently, the ratios versus the geometric means.

Results

Validation of a CAD tool based on measurement of average fluence rate

Table 1 compares average CAD-predicted fluence rates in the experimental chamber with measurement-based estimates of fluence rate using three sensing devices: (1) a flat sensor, (2) a cylindrical sensor, and (3) a chemical actinometer. The percentage difference using the measured average fluence rate as a basis was less than 10% for all measurement methods used. A paired t-test was used to test the null hypothesis that the average difference between the measured fluence rate and CAD-predicted fluence rate at specific locations was equal to zero. As shown in Table 1, the null hypothesis could not be rejected at 95% confidence for the flat sensor ($p = 0.62$ for $n = 258$ measurements) or chemical actinometry ($p = 0.12$; $n = 97$), but it was rejected ($p = 0.013$; $n = 258$) using the cylindrical sensor.

Table 1 also compares average CAD-predicted fluence rates in a homeless shelter with measurements using the cylindrical sensor. Initially, agreement was rather poor. For the "original" predictions shown in Table 1, the percentage difference was 50% of the measured average. Based on a paired t-test, the null hypothesis was rejected at very high confidence ($p = 1.3 \times 10^{-25}$ for $n = 1100$ measurements).

In order to try to explain this discrepancy, additional irradiance measurements were made that were independent of the measurements being compared to the CAD-predicted fluence rates; for these independent measurements, the maximum irradiance was measured at a distance of 3 ft (0.914 m) from each face of the fixtures. These irradiances were used as benchmarks for the UV power output of the fixtures. As shown in Table 2, these benchmarks

Downloaded by [University of Colorado at Boulder Libraries] at 14:01 15 August 2012

Table 1. Comparison of average measured and CAD-predicted fluence rates.

Venue and sensor type	Number pairs	Average fluence rate, μW/cm^2		Percentage difference[b]	Average difference, uW/cm^2		Paired *t*-test: reject null hypothesis?[c]
		Measured	Predicted[a]		Measured − predicted	95% confidence interval	
Experimental chamber:							
Cylindrical sensor	258	19.4	21.2	–9.3%	–1.8	±1.4	Yes ($p = 0.013$)
Flat sensor	258	20.7	20.4	1.3%	0.26	±1.03	No ($p = 0.62$)
Chemical actinometry	97	44.3	41.0	7.4%	3.3	±4.1	No ($p = 0.12$)
Homeless shelter							
Cylindrical sensor							
Original	1100	7.20	10.8	50%	−3.6	±0.66	Yes ($p = 1.3 \times 10^{-25}$)
Corrected[d]	1100	7.20	7.18	0.28%	0.020	±0.47	No ($p = 0.93$)

[a]Reflectivity was assumed to be 10%, except when measurements were made with the flat sensor when the reflectivity was assumed to be 0%.

[b]Percentage difference is defined as 100 (*Measured* − *Predicted*)/*Measured*.

[c]Null hypothesis is no difference between measured and predicted fluence rates at 95% confidence.

[d]Because the aged UV fixtures in the homeless shelter had low UV output, the predicted fluence rate for each face of the three pendant fixtures were multiplied by the appropriate correction factor listed in Table 2.

Downloaded by [University of Colorado at Boulder Libraries] at 14:01 15 August 2012

Table 2. Maximum irradiances at 3 ft (0.914 m) from faces of UV fixtures in homeless shelter.

Fixture/face[a]	Height above floor, in. (m)	Maximum irradiance, μW/cm^2	Correction factor[b]
#1/North	1109 (2.77)	229	00.84
#1/South	1108 (2.74)	190	00.69
#2/North	1109 (2.77)	195	00.71
#2/South	1109 (2.77)	154	00.56
#3/North	1104 (2.64)	178	00.65
#3/South	1106 (2.69)	170	00.62

[a]See Figure 2.

[b]Maximum measured irradiance divided by 274 μW/cm^2 (2.74 W/m^2), which was predicted by the CAD tool based on gonioradiometry.

varied from 154 μW/cm^2 to 229 μW/cm^2 (1.54 W/m^2 to 2.29 W/m^2) for each of the two faces of the homeless shelter's three two-way Hygeaire model LIND 24-EVO-PM. However, based on gonioradiometric measurements, the CAD tool predicted a maximum irradiance of 274 μW/cm^2 (2.74 W/m^2) at a distance of 3 ft (0.914 m) from each face of these three fixtures. This predicted maximum irradiance was significantly larger than all of the measured maximum irradiances. Lamp, ballast, and fixture performance degrade over time due to many factors, so the fixtures' loss of UV power was not surprising. Correction factors for each face of the three fixtures, which are listed in Table 2, were calculated by dividing the maximum measured irradiance at a distance of 3 ft (0.914 m) from each face of the fixture by the maximum predicted irradiance of 274 μW/cm^2 (2.74 W/m^2). For each fixture face, the gonioradiometric measurements were then multiplied by this correction factor. These corrected gonioradiometric measurements were used as input to the CAD tool for the purpose of predicting the fluence rate field attributable to each face of the three fixtures.

After applying these correction factors, the percentage difference between the average predicted fluence rates and average measured fluence rates in the homeless shelter was equal to 0.28%. A paired *t*-test did not reject the hypothesis that the average difference between measured and CAD-predicted fluence rates was equal to zero ($p = 0.93$ for $n = 1100$).

Comparison of measured and predicted fluence rates at specific locations

Figures 3, 4, and 5 are Bland–Altman plots comparing measured and CAD-predicted fluence rates at specific locations in the experimental chamber using the cylindrical sensor, flat sensor, and chemical actinometer, respectively. Figure 6, which is based on the corrected fluence rates, is the Bland–Altman plot for the sitting room of the homeless shelter using the cylindrical sensor. In these figures, the ratio of the measured (M) to predicted (P) fluence rates is plotted on the vertical axis versus their geometric mean on the horizontal axis; that is, M/P versus $\sqrt{MP}$. The bias line, which is labeled as such in Figure 3 but not on the other figures, on average, gives the ratio of measured to predicted fluence rates as a function of the geometric mean fluence rate. The bias line crosses the horizontal axis when, on average, the measured and predicted fluence rates are equal; that is, their ratio is equal to one. In Figures 3–6, this ratio was equal to one when the geometric mean fluence rates were 51, 38, 37, and 19 μW/cm^2 (510, 380, 370, and 190 mW/m^2), respectively. However, when the ratio, on average, was equal to one, 95% of the ratios were between 0.52 and 1.9, 0.47 and 2.1, 0.52 and 1.9, or 0.44 and 2.3, respectively. At lower fluence rates, the ratio tended to be less than one, whereas at higher fluence rates, the ratio tended to be greater than one.

Comparison of measured UV power output of fixtures

Gonioradiometry was done on the three types of UV fixtures used in this study specifically because it is a necessary input for predicting fluence rate with the CAD tool. An added benefit of these measurements is that UV power output of these fixtures can be accurately determined. For the three fixture types, UV power output, electrical power input, and efficiency based on UV power output of the lamps or electrical power input to the fixture are given in

Downloaded by [University of Colorado at Boulder Libraries] at 14:01 15 August 2012

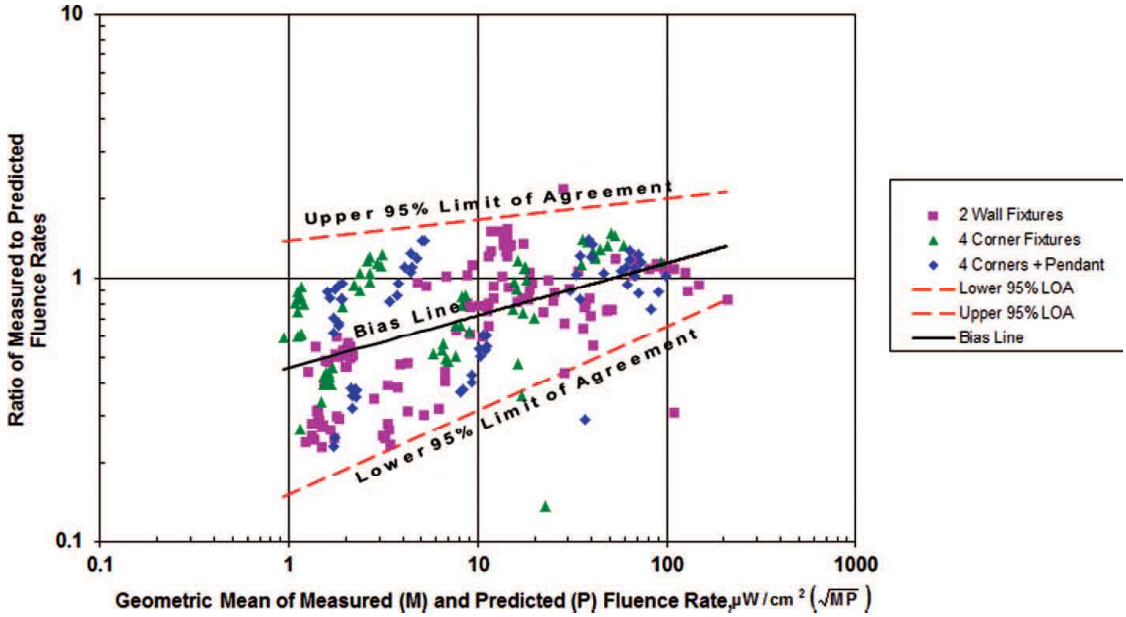

Figure 3. Comparison of measured and predicted fluence rate for cylindrical sensor in experimental room (color figure available online).

Table 3. The Lumalier model PM-418 pendant fixture had the highest UV power output of the three fixtures tested (0.59 W), but its efficiency based on either UV output of the lamp or electrical input was only about half that of the Hygeaire model LIND-EVO wall fixture.

The UV power output of 0.473 W for the Hygeaire model LIND 24-EVO fixture is in excellent agreement with the 0.45 W reported elsewhere (Rudnick and First 2007), which was based on a different measurement methodology. The UV power output of 0.128 W for the Lumalier model

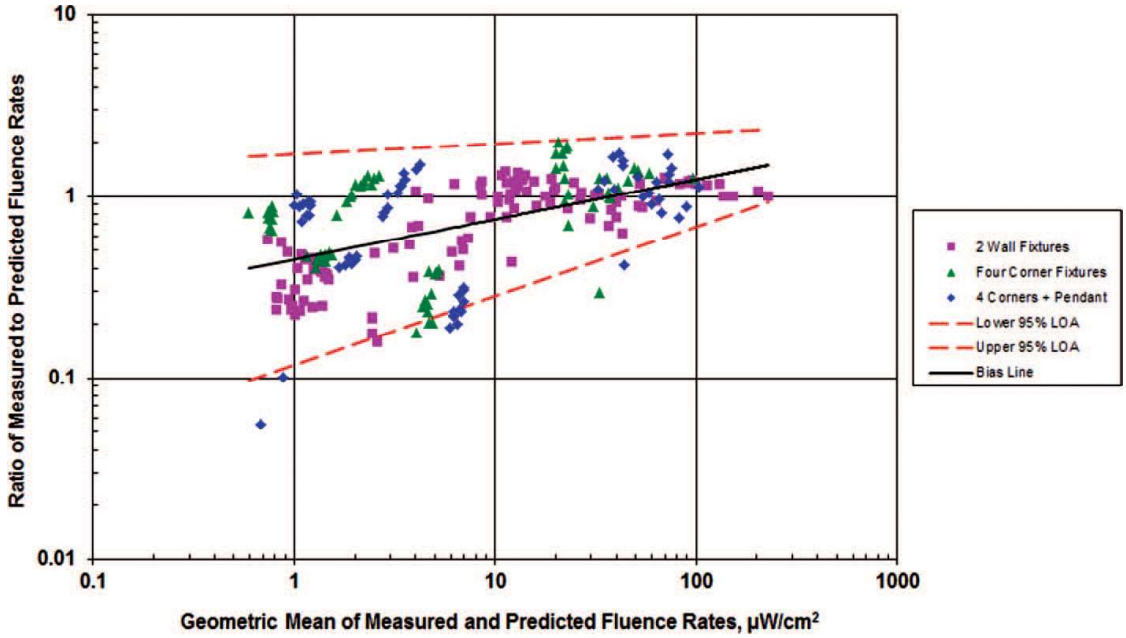

Figure 4. Comparison of predicted and measured fluence rates for flat sensor in experimental room (color figure available online).

Downloaded by [University of Colorado at Boulder Libraries] at 14:01 15 August 2012

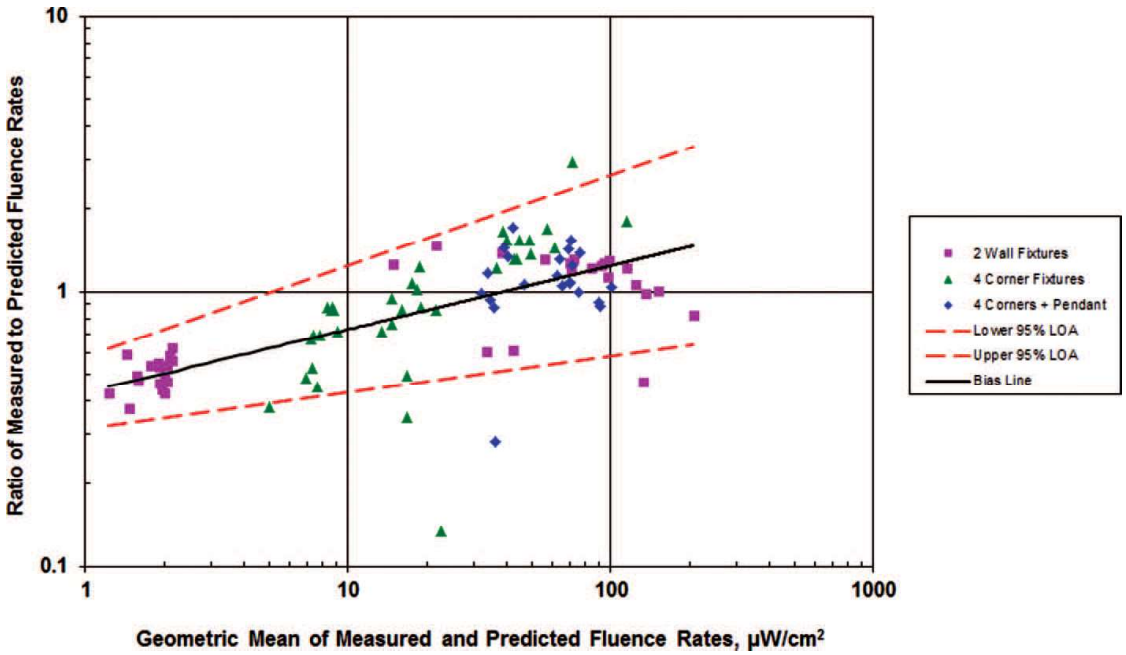

Figure 5. Comparison of measured and predicted fluence rates by actinometry in experimental room (color figure available online).

CM-218 corner fixture, however, is in rather poor agreement with the estimated 0.05 W reported elsewhere (Rudnick and First 2007), which was based on an assumption that may be invalid. The estimate of 0.05 W was based on measurements made by Dumyahn and First (1999) that gave a UV power output of 0.025 W for an earlier model Lumalier corner fixture containing one 18-W folded compact lamp that was believed to be essentially the same as the Lumalier model CM-218 corner fixture except that the latter fixture contained two 18-W folded compact lamps.

Discussion

Comparison of measured and predicted average fluence rates

As originally conceived, the primary objective was to validate CAD predictions of average fluence rate in the irradiated zone of a room equipped with upper-room UVGI by comparing them to measurements made in an experimental chamber where conditions could be well controlled. In addition, an attempt was made to confirm this validation in a

Table 3. UV output of fixtures based on gonioradiometry.

Fixture type	Manufacturer	Model	UV power output, W		Electrical power input, W	Efficiency	
			Lamps[a]	Fixture		$UV_{fixture}/UV_{lamp}$[a]	$UV_{fixture}/Electricity$
Wall	Atlantic Ultraviolet	Hygeaire Model LIND 24-EVO	8.5	0.473	26.0	5.56%	1.82%
Corner	Commercial Lighting Design	Lumalier Model CM-218	11	0.128	36.6	1.16%	0.350%
Pendant	Commercial Lighting Design	Lumalier Model PM-418	22	0.591	68.3	2.68%	0.865%

[a]Nominal.

Downloaded by [University of Colorado at Boulder Libraries] at 14:01 15 August 2012

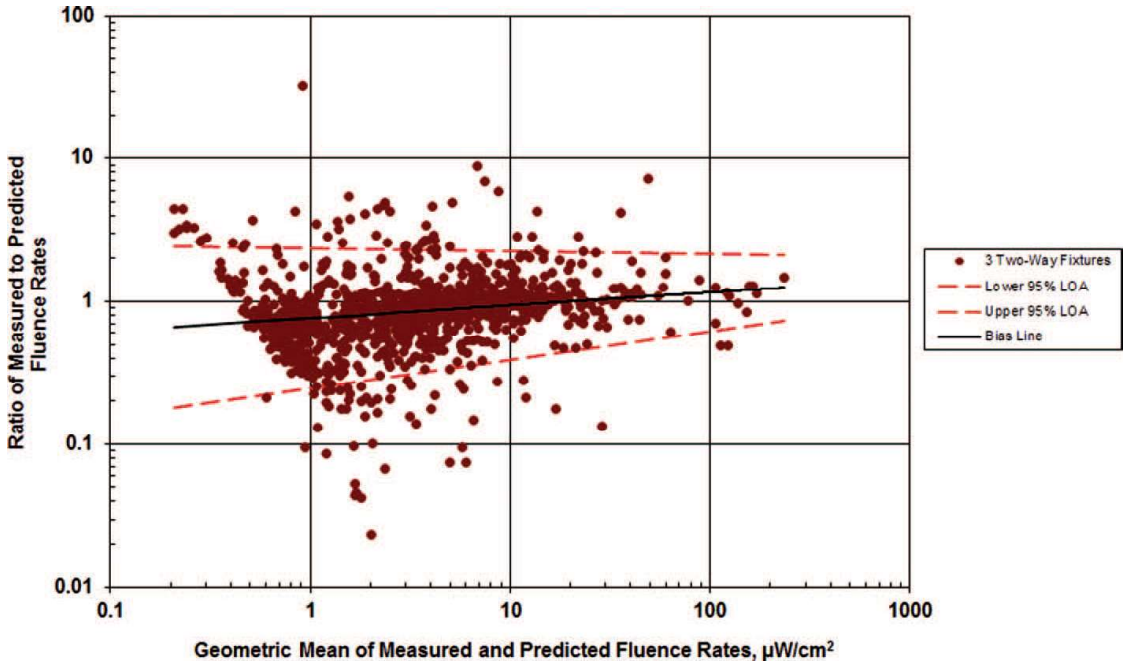

Figure 6. Comparison of predicted and cylindrical-sensor measured fluence rates in sitting room of New York City homeless shelter (color figure available online).

real-world location where upper-room UVGI was currently in use. The sitting room of a homeless shelter where UVGI fixtures had been in continuous operation for over 7 years was chosen for this confirmation. As shown in Table 1, for both the experimental chamber and the homeless shelter, measured and predicted average fluence rates were in excellent agreement for the three types of sensors used, although a few caveats must be noted. In this study's experimental chamber, the predicted and measured average fluence rates were within 1.3% for the flat sensor, 7.4%, for chemical actinometry, and 9.3% for the cylindrical sensor. Based on the outcome of paired *t*-tests, also shown in Table 1, the null hypothesis—the premise that the difference between the measured and predicted fluence rates was equal to zero—could not be rejected at 95% confidence for the flat sensor or chemical actinometry; however, it was rejected for the cylindrical sensor ($p = 0.013$), in part, because the number of pairs was fairly large ($n = 258$). For practical purposes, however, a 9.3% difference between predicted and measured values is nevertheless a reasonably accurate prediction. In the sitting room of the homeless shelter, the predicted and measured average fluence rates were within only 0.28% after predictions were corrected for the reduced output of the relatively old fixtures in use at the shelter. Thus, the CAD tool appears to be able to predict average fluence rate fairly well, and it should, therefore, be helpful in determining the number and type of UV fixtures necessary for the control of airborne transmission of infectious particles in a room.

One caveat, however, is that for the homeless shelter, the original predicted average fluence rate was almost 50% greater than the measured average fluence rate. By taking benchmark readings, it could be shown that all of the fixtures, which had been in continuous use in the homeless shelter for more than 7 years, were putting out less UV radiation than newer fixtures. The CAD predictions were then scaled to account for the differences in UV output of these fixtures, resulting in the 0.28% difference in measured and predicted values, although admittedly this is much better agreement than could be realistically expected. Although no specific reasons were found for the reduced output of these fixtures, the use of these fixtures continuously for over 7 years may have been the cause. Improvements in fixture design may also have taken place without the model number being changed. The fixtures used in the experimental chamber were not benchmarked because they were all relatively new and had very limited usage. When attempting to benchmark

Downloaded by [University of Colorado at Boulder Libraries] at 14:01 15 August 2012

these fixtures later, for various reasons it was not possible. In retrospect, it appears to be good practice to benchmark all fixtures, because no two fixtures are identical, particularly after heavy usage; then, CAD predictions can be adjusted appropriately. Even if prediction of average fluence rate is not being made, benchmarking fixtures a few weeks after installation and periodically thereafter will provide assurance that fixtures are operating properly.

Another concern was that the exact reflectivities of the surfaces in the experimental chamber or in the sitting room of the homeless shelter were not known. Measurements on the walls and ceiling in the experimental chamber indicated that their reflectivity was less than 10%, and this value is also reasonable for most paints (Ulrich and Evans 1976). As shown in Table 2, the CAD-predicted average fluence rate for 264 test sites in the experimental chamber was 20.4 μW/cm^2 (204 mW/m^2) for 0% reflectivity; increasing reflectivity to 10% resulted in a prediction of 21.2 μW/cm^2 (212 mW/m^2), only a 3.9% increase in fluence rate. Thus, accurate knowledge of reflectivity is not very important when reflectivity is less than 10%. In addition, as long as reflectivity is underestimated, the prediction of fluence rate in the upper room will err on the conservative side.

As shown in Table 2, the predicted average fluence rate assuming that chamber surfaces had 0% reflectivity was only 1.4% higher than the measured average fluence rate using the flat sensor. If reflections were significant, then agreement would be expected to be much poorer. Thus, when surface reflectively is not significant—or at least not greater than 10%—it is reasonable to assume that fluence rate can be estimated reasonably well by summing the planar irradiances attributable to each fixture while other fixtures are turned off.

Comparison of measured and predicted fluence rates at specific locations

An algorithm that can predict accurately the effectiveness of upper-room UVGI requires three separate physical models.

1. A model that can predict the location of infectious particles over time is essential. Computational fluid dynamics (CFD) has the capability to predict a particle's pathway.
2. A model that can predict the fluence rate at any desired location, such as the CAD tool described above, is also necessary. Together, CFD and the CAD tool have the capability to predict the UV dose, that is, the total UV energy impinging on an infectious particle from when it enters the room to when it is inactivated or exits the room.
3. A model that predicts the probability that an infectious particle will be inactivated based on the UV dose received is also required.

In order to determine if the CAD tool was adequate to serve as the second model listed above, experimental measurements and predictions from the CAD tool at specific locations in the upper room needed to be compared. The Bland–Altman plots in Figures 3 through 6 serve this purpose. All of these plots show two similarities: (1) the bias line always has a positive slope; that is, the ratio of measured to predicted fluence rate tends to increase as fluence rate increases and (2) the bias line always crosses the horizontal axis; thus, at an intermediate value of fluence rate, the measured and predicted fluence rates are, on average, equal. The fluence rate at which the measured and predicted fluence rates are equal varied from 19 μW/cm^2 to 51 μW/cm^2 (190 mW/m^2 to 510 mW/m^2), depending on measurement method. In this range of fluence rate, the CAD tool is most accurate, although the rather wide 95% LOA suggests that it is not really very accurate. The 95% LOA for all methods of measurement ranged from a ratio of measured to predicted fluence rate of approximately 0.5 to 2; that is, 95% of the ratios were spread out over a four-fold range. Therefore, prediction or measurement of fluence rate at a specific location, or perhaps both, is prone to rather large errors, and the CAD tool should be used in conjunction with CFD software with caution at the present time.

Other than deficiencies in the CAD tool (see Appendix), measurement equipment, and calibration of instrumentation, there are a number of reasons that could cause a predicted fluence rate at a specific test site to not match a measured fluence rate.

1. Due to the louvers, the irradiance field from the UV fixture contains discontinuities; that is, the irradiance can change very abruptly at a particular location (Rudnick 2001). The closer the measurement point is to the fixture, the more significant the discontinuity can be.

Downloaded by [University of Colorado at Boulder Libraries] at 14:01 15 August 2012

2. The various sensors have dissimilar sizes and shapes, and they must be oriented differently; thus, it is only possible to estimate the fluence rate at a specific point in space. In addition, the average fluence rate over the surface area of any of the sensors is what is really being measured.
3. The louvers slant slightly upward by design, so that the UV beam will rise slightly in the range of 3° to 7°. This angle at which the beam rises, however, can vary, because the fixture may not be perfectly leveled or due to variation from one fixture to another. The farther the measurement point is from a fixture, the greater the percentage error is likely to be.

Thus, in addition to the usual measurement errors, small errors in the geometric relationship between the fixture and measurement location can have a significant impact on the agreement between measurements and CAD predictions. Further work needs to be done to determine whether this geometric relationship is the primary cause of the poor agreement between measured and predicted fluence rates that were observed at a specific test site.

Comparison of measured UV power output of fixtures

The UV power output for the three fixtures used in this study varied considerably—0.13 W for the Lumalier corner fixture, 0.47 W for the Hygeaire wall fixture, and 0.59 W for the Lumalier pendant fixture. For purposes of designing a UVGI installation, these values are crucial because the UV power exiting a fixture is probably the best single-number characterization of a fixture's potential for disinfection of upper-room air (Rudnick 2001). However, more important for choosing a UV fixture, perhaps, is the overall efficiency of the fixture; that is, the percentage of the electrical input that exits the fixture as UV radiation. The Hygeaire wall fixture with an overall efficiency of 1.8% is more than twice as efficient as the Lumalier pendant fixture and more than five times as efficient as the Lumalier corner fixture.

Conclusions

Based on experimental measurements in a room-size chamber using three different types of UV sensors and in a homeless shelter employing the simplest of the three sensors to use, validation was provided that a newly modified CAD tool originally designed for interior lighting could be used to make reasonably accurate predictions of average fluence rate in the irradiated zone of a room with upper-room UVGI installed. This capability should be useful for providing help in determining dosing requirements for upper-room UVGI, that is, determining the number and type of UV fixtures necessary for the control of airborne transmission of infectious particles in a room. This CAD tool, however, did rather poorly when predicting fluence rate at a specific location in a room. This failure was unfortunate because the successful mating of CFD with the CAD tool has the potential to predict the effectiveness of upper-room UVGI over a wide range of conditions. Further work is required to determine why predicted and measured fluence rates at a specific location were not more comparable.

Use of the CAD tool requires gonioradiometric measurements to be made in the laboratory on representative UV fixtures. Although it was not an objective of this study, it was found that the three commercial UV fixtures evaluated in this study by gonioradiometry have significant differences in efficiency, that is, the ratio of the fixture's UV power output to the electrical input to the fixture. One of these fixtures has an efficiency that was more than five times that of one of the other fixtures. Thus, there is a need for commercial UV fixtures to be subjected to standard tests to evaluate their efficiency, which would then allow end users to select UV fixtures that do not needlessly waste electricity.

Acknowledgments

The authors thank the New York State Energy Research and Development Authority (NYSERDA) for supporting this work (Project 9450). Thanks also go to David DiLaura for his help in modifying the Visual program for UVGI and the committee that helped plan this research project, which, in addition to the authors, included Robert Angelo, Hilary Boehme, William Chaisson, Charles Dunn, Jr., Randall King, and Paul Minor.

References

Altman, D.G., and J.M. Bland. 1983. Measurement in medicine: the analysis of method comparison studies. *Statistician* 32:307–17.

Björn, L.O. 1995. Estimation of fluence rate from irradiance measurements with a cosine-corrected sensor. *Journal of Photochemistry and Photobiology B: Biology* 29(2–3):179–83.

Downloaded by [University of Colorado at Boulder Libraries] at 14:01 15 August 2012

Bland, J.M., and D.G. Altman. 1986. Statistical methods for assessing agreement between two methods of clinical measurement. *Lancet* i: 307–10.

Bland, J.M., and D.G. Altman. 1999. Measuring agreement in method comparison studies. *Statistical Methods in Medical Research* 8:135–60.

Brickner, P.W., R.L. Vincent, M. First, E. Nardell, M. Murray, and W. Kaufman. 2003. The application of ultraviolet germicidal irradiation to control transmission of airborne disease: Bioterrorism countermeasure. *Public Health Reports* 118:99–113.

DiLaura, D.L. 1982. On the simplification of radiative transfer calculations. *Journal of the Illuminating Engineering Society* 12(1):12–16.

DiLaura, D.L. 1996. Nondiffuse radiative transfer 2: Planar area sources and receivers. *Journal of the Illuminating Engineering Society* 25(2):140–49.

DiLaura, D.L., and J. Quinlan. 1995. Non-diffuse radiative transfer 1: Area sources and point receivers. *Journal of the Illuminating Engineering Society* 24(2):102–13.

Dumyahn, T., and M.W. First. 1999. Characterization of ultraviolet upper room air disinfection devices. *American Industrial Hygiene Association Journal* 60:219–27.

Dye, C., and K. Floyd. 2006. *Disease Control Priorities in Developing Countries,* 2nd ed., Tuberculosis, D.T. Jamison, J.G. Breman, A.R. Measham, G. Alleyne, M. Claeson, D.B. Evans, P. Jha, A. Mills, P. Musgrove, eds., chap. 16, PubMed PMID 21250305. Washington, DC: World Bank.

Escombe, A.R., D.A. Moore, R.H. Gilman, M. Navincopa, E. Ticona, B. Mitchell, C. Noakes, C. Martinez, P. Sheen, R. Ramirez, W. Quino, A. Gonzalez, J.S. Friedland, and C.A.Evans. 2009. Upper-room ultraviolet light and negative air ionization to prevent tuberculosis transmission. *PLoS Medicine* 6:e43.

First, M.W., S.N. Rudnick, K.F. Banahan, R.L. Vincent, and P.W. Brickner. 2007. Fundamental factors affecting upper-room ultraviolet germicidal irradiation—Part I. *Experimental. Journal of Occupational and Environmental Hygiene* 4(5):321–31.

Gandhi, N.R., A. Moll, A.W. Sturm, R. Pawinski, T. Govender, U. Lalloo, K. Zeller, J. Andrews, and G. Friedland. 2006. Extensively drug-resistant tuberculosis as a cause of death in patients co-infected with tuberculosis and HIV in a rural area of South Africa. *Lancet* 368:1575–80.

IESNA Testing Procedures Committee. 1998. *Photometric testing of indoor fluorescent luminaires*. IESNA LM-41–98. Illuminating Engineering Society of North America, New York.

IESNA Testing Procedures Committee. 2001. *Goniophotometer types and photometric coordinates*. IESNA LM-75–01. Illuminating Engineering Society of North America, New York.

IESNA Testing Procedures Committee. 2002. Standard file format for electronic transfer of photometric data and related information. ANSI/IESNA LM-63–02. Illuminating Engineering Society of North America, New York.

Lorensen, W.E., and H.E. Cline. 1987. Marching cubes: A high resolution 3D surface construction algorithm. *Computer Graphics* 21(4):163–9.

Miller, S.L., M. Hernandez, K. Fennelly, J. Martyny, J. Macher, E. Kujundzic, P. Xu, P. Fabian, J. Peccia, and C. Howard. 2002. Efficacy of ultraviolet irradiation in controlling the spread of tuberculosis. Final Report CDC/NIOSH Contract No. 200–97-2602, NTIS PB2003–103816, University of Colorado, Boulder, CO.

NIOSH. 2009. Engineering control for tuberculosis: Basic upper-room ultraviolet germicidal irradiation guidelines for healthcare settings. DHHS Publication No. 2009–105. National Institute for Occupational Safety and Health, Cincinnati OH.

O'Brien, P.F. 1955. Interreflections in rooms by a network method. *Journal of the Optical Society of America* 45(6):419–24.

O'Brien, P.F., and J.A. Howard. 1959. Predetermination of luminances by finite difference equations. *Illuminating Engineering* 54(4):209–81.

Pantelic, J., G.N. Sze To, K.W. Tham, C.Y.H Chao, and Y.C.M. Khoo. 2009. Personalized ventilation as a control measure for airborne transmissible disease spread. *Journal of Royal Society Interface* 6:S715–26.

Rahn, R.O. 1997. Potassium iodide as a chemical actinometer of 254 nanometer radiation: Use of iodate as an electron scavenger. *Photochemistry and Photobiology* 66:450–5.

Rahn, R.O., and S. Echols. 2010. Iodide/iodate chemical actinometry using spherical vessels for radiation exposure as well as for monitoring absorbance changes. *Photochemistry and Photobiology* 86(4):990–93.

Rahn, R.O., P. Xu, and S.L. Miller. 1999. Dosimetry of room-air germicidal (254 nm) radiation using spherical actinometry. *Photochemistry and Photobiology* 70(3):314–8.

Riley, R.L., and F. O'Grady. 1961. *Airborne Infection—Transmission and Control*. New York: Macmillan.

Roy, C.J., and D.K. Milton 2004. Airborne transmission of communicable infection—the elusive pathway. *New England Journal of Medicine* 350:1710–2.

Rudnick, S.N. 2001. Predicting the ultraviolet radiation distribution in a room with multi-louvered germicidal fixtures. *American Industrial Hygiene Association Journal* 62:434–45.

Rudnick, S.N., and M.W. First. 2007. Fundamental factors affecting upper-room ultraviolet germicidal irradiation—Part II: Predicting effectiveness. *Journal of Occupational and Environmental Hygiene* 4(5):352–62.

Santoro, S. 1996. *Calculating flux transferred accounting for intervening objects*. Master's thesis, University of Colorado at Boulder, Boulder, CO.

Schafer, M.P., E. Kujundzic, C.E. Moss, and S.L. Miller. 2008. Method for estimating ultraviolet germicidal fluence rates in a hospital room. *Infection Control and Hospital Epidemiology* 29(11):1042–47.

Ulrich, O.A., and R.M. Evans. 1976. Ultraviolet reflectance of paints. AWS ULR-76. American Welding Society, Miami, FL.

Wells, W.F. 1955. *Airborne Contagion and Air Hygiene.* Cambridge, MA: Harvard University Press.

Xu, P., E. Kujundzic, J. Peccia, M.P. Schafer, G. Moss, M. Hernandez, and S. L. Miller. 2005. Impact of environmental factors on efficacy of upper-room air ultraviolet germicidal irradiation for inactivating airborne mycobacteria. *Environmental Science and Technology* 39:9656–64.

Xu, P., J. Peccia, P. Fabian, J.W. Martyny, K.P. Fennelly, M. Hernandez, and S.L. Miller. 2003. Efficacy of ultraviolet

germicidal irradiation of upper-room air in inactivating airborne bacterial spores and mycobacteria in full-scale studies. *Atmospheric Environment* 37: 405–19.

Zhang, J., R. Levin, R. Angelo, R. Vincent, P. Brickner, P. Ngai, and E. Nardell. 2012. A radiometry protocol for UVGI fixtures using a moving-mirror type gonioradiometer. *Journal of Occupational and Environmental Health* 9(3):140–8.

Downloaded by [University of Colorado at Boulder Libraries] at 14:01 15 August 2012

Appendix: Prediction of fluence rate using a CAD tool

Visual™(Acuity Brands Lighting, Conyers, GA), which is application software designed for analysis of architectural lighting layouts, is provided to the lighting community for use in designing and specifying lighting systems. Visual's ability to predict physics-based point illuminance values in space along with its robust set of visualization and analysis tools make it a suitable candidate for the incorporation of UVGI calculations. Only minor changes were required to extend Visual's calculation engine to UVGI.

Visual is lighting software and, as such, is built around the quantities and units of measurement used in illuminating engineering, such as lumens, luminous intensity (candela), luminance, and illuminance. All of these terms are specific to the measurement of visible light. For use with UVGI, Visual was modified to use the corresponding radiometric analogs where appropriate. For example, watts are substituted for lumens, radiant intensity for luminous intensity, radiance for luminance, and irradiance or fluence rate for illuminance.

The calculation of irradiance at a point in space is one of Visual's primary functions. Point irradiance can be considered as composed of two separate components: (1) a direct component due to line-of-sight flux from all radiant sources and (2) an interreflected component due to flux reflecting between surfaces in the space and ultimately arriving at the point. Visual determines the direct component of irradiance using a contour integration method (DiLaura and Quinlan 1995). This method allows Visual to account very accurately for the total flux emitted by a source, as opposed to earlier approaches that usually involved discretizing each source into small pieces in order to maintain far-field integrity. Visual determines the interreflected component of irradiance by using the principles of radiant energy transfer to set up and solve a system of linear equations (O'Brien 1955; O'Brien and Howare 1959; DiLaura 1982, 1996; Santoro 1996). This approach is distinct from the common approach of ray tracing. Although both approaches are physics based, there are benefits and trade-offs to each method. In general, radiant transfer engines are much faster than ray tracing, but particular assumptions about the physical properties of the system must be met. The three primary assumptions are as follows: (1) each surface is a perfectly diffuse reflector, (2) the reflected radiance of each surface is homogeneous, and (3) each surface exhibits a constant spectral reflectance through the spectral region of interest. Fortunately, the requirements for radiative transfer are reasonable and easily met for most architectural lighting situations and for UVGI, so the radiative transfer approach is appropriate. It does mean, however, that Visual cannot accurately model specular surfaces, such as a mirror or polished stone.

The calculation of fluence rate required some modification of the calculation engine. This quantity has a lighting analog, spherical illuminance, but this latter parameter is not used in practice, and so was not calculated by Visual. The modifications, however, are straightforward, as fluence rate is the general case of directional irradiance. Equations used for determination of directional irradiance were re-derived without consideration of the angle of incident flux, with the end result being fluence rate. Additionally, a new visualization technique was added to the modeling environment to interpret the results of the fluence rate calculation. A volumetric rendering technique, "Marching Cubes" (Lorensen and Cline 1987), was implemented so that the user can visualize the volume of space that is irradiated by a UVGI system and obtain metrics that determine the total percentage of the upper-room volume that is above a threshold fluence rate level. Another visualization tool added specifically for UVGI analysis is the ability to scale a radiometric indicatrix, displayed with each UVGI fixture, to a given fluence rate threshold. This effectively shows the "kill volume" produced by each fixture and aids in the initial layout of the system.

A final and significant limitation to Visual's predictive ability is the nature and quality of the radiometric data that the software uses to model fixture output. The convention in the lighting industry is to use "far-field" photometric data, which is generally only acceptably accurate for discrete point illuminance calculations at distances that are more than five times the largest dimension of the fixture

(effectively modeling the fixture as a point source). This limitation of photometry means that Visual cannot account for near-field photometric effects and must treat all luminaires as homogeneous over their luminous extent. For example, the near-field shadowing effect of the baffles of a UV fixture is not modeled by Visual and will result in extreme discrepancies between predicted irradiances or fluence rates and real-world measurements. There are approaches that can mitigate or eliminate this problem (e.g., application distance photometry, luminance field photometry, and luminance scan photometry), but none of these approaches has yet been accepted into practice by the lighting industry.

Gonioradiometric evaluation of representative UV fixtures

A new protocol for gonioradiometry of UV fixtures was developed based on standard methods for photometry and reporting of general fluorescent lighting fixture data (IESNA Testing Procedures Committee 1998). A moving-mirror, Type-C goniophotometer (Independent Testing Laboratories, Boulder, CO) was equipped with a specialized UVGI reflective mirror (Milcure 1000 aluminum reflector sheet, Miltec UV, Stevensville, MD) and GigaHertz-Optik model P9710 optometer with model UV-3718–2 flat UV sensor (Puchheim, Germany). Each UV fixture tested was mounted in the radiometric center of the gonioradiometer, and the mirror was mechanically rotated around the fixture while reflecting the radiant power to the UV sensor located at a distance equal to five or more times the largest dimension of the fixture and at the same height as the radiometric center. A computer recorded these three-dimensional UV data points at a series of predetermined vertical and horizontal angles (IESNA Testing Procedures Committee 2001). These data were recorded in an IES electronic file format (IESNA Testing Procedures Committee 2002), which was capable of being accessed by Visual software.

Downloaded by [University of Colorado at Boulder Libraries] at 14:01 15 August 2012

View publication stats